New Journal of Chemistry: NJ-ART-08-2013-00099.R3

Supporting Information

Structure and properties of metal complexes of a pyridine based oxazolidinone synthesized by atmospheric CO_2 fixation

Amrita Sarkar,[a] Sudipta Bhattacharyya,[a] Suman Kr Dey,[a] Subhendu Karmakar[a] and Arindam Mukherjee*[a]

Department of Chemical Sciences Indian Institute of Science Education & Research Kolkata, Mohanpur Campus, P.O.- BCKV Main Campus, District- Nadia, Pin- 741252, INDIA.

Fax: (+91)033-25873118; Tel: (+91)033-25873121; E-mail: a.mukherjee@iiserkol.ac.in

Contents:

Table S1 Crystallographic data and structure refinement parameters for complexes **1-3.**

	1	**2**	**3**[a]
Empirical formula	C_{18} H_{20} Cl_2 N_4 O_{12} Cu	C_{11} H_{17} Cl_2 N_2 $O_{3.5}$ Pt S	C_{18} H_{20} Cl_2 N_4 O_4 Pd
F_w (g mol^{-1})	618.83	531.32	533.68
Temperature(K)	100(2)	100(2)	100(2)
Crystal system	Monoclinic	Triclinic	Monoclinic
space group	*P*2(1)/c	*P*-1	*P*2(1)
Crystal size/mm	0.65 x 0.32 x 0.17	0.68 x 0.34 x 0.15	0.54x0.33x0.19
a(Å)	9.0019(4)	8.128(17)	8.239(2)
b(Å)	8.0278 (3)	13.281(3)	13.553(2)
c(Å)	16.0297(7)	14.755(3)	9.605(2)
α(°)	90	97.093(4)	90.00
β(°)	99.170(2)	94.263(4)	106.362(3)
γ(°)	90	96.436(4)	90.00
V($Å^3$)	1143.6(8)	1564.3(6)	1029.1(3)
Z	2	4	2
D_c (g/cm^{-3})	1.797	2.256	1.722
μ(mm^{-1})	1.263	9.455	1.194
F(000)	560	1012	536
Limiting indices	-12<h<12, -9<k<10, -21<l<18	-6<h<10, -16<k<16, -18<l<18	-10<h<10, -17<k<17, -12<l<12
Reflections collected	9539	23983	16687
Flack parameter	-	-	0.45(6)
Unique Reflections/R_{int}	2850/ 0.0341	6388/ 0.0365	4712/ 0.0429
Data / restraints / parameters	2850 / 0 / 169	6388 / 0 / 375	4712 / 1 / 263
Goodness-of-fit[b] on F^2	1.033	1.047	
R_1[c], wR_2[d] [I>2σ(I)]	0.0420/ 0.1092	0.0192/ 0.0495	
R_1,wR_2 (all data)	0.0610/ 0.1208	0.0211/ 0.0507	
$\Delta\rho_{max/min}$ /e $Å^{-3}$	0.869 / -0.599	1.370/ -1.376	

[a] it was not possible to derive a fully acceptable structure hence the structure is not published here. [b] Goodness-of-fit=$[\Sigma w(F_o^2 - F_c^2)^2]/(N_{reflection} - N_{params})]^{1/2}$, based on all data. [c] $R_1 = \Sigma (|F_o| - |F_c|)/|F_o|$. [d] $wR_2 = [R [\Sigma (F_o^2 - F_c^2)^2]/R[\Sigma(F_o^2)^2]]^{1/2}$.

Table S2 Screening of solvent for the reaction of 4-bromoanisole and phenylboronic acid[a]

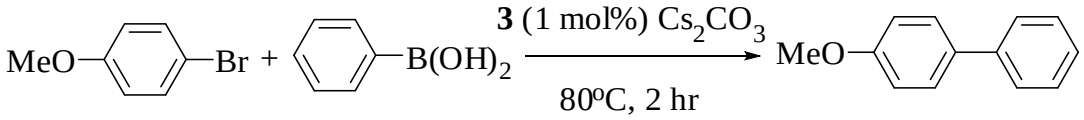

Entry	Solvent	% Yield[b]
1	H_2O	90
2	EtOH	92
3	MeCN	86

[a]Reaction conditions: 4-bromoanisole (0.093 g, 0.5 mmol), phenylboronic acid (0.0915 g, 0.75 mmol), Cs_2CO_3 (1.5 mmol), [b]Isolated yield after column chromatography.

Scheme S1

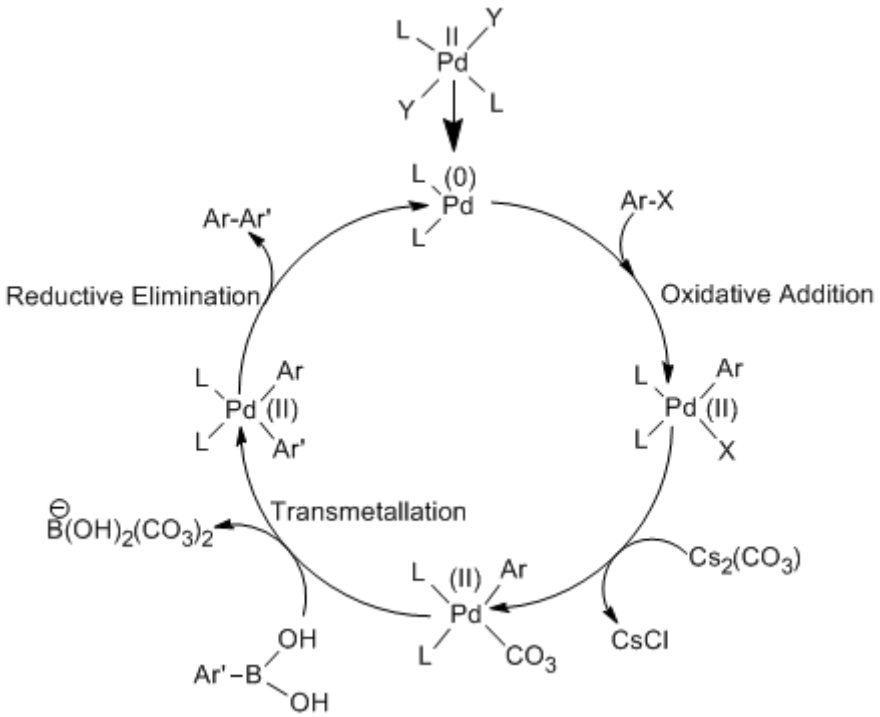

Scheme S1 Proposed catalytic cycle for Suzuki-Miyaura Coupling by complex **3** in presence of base.

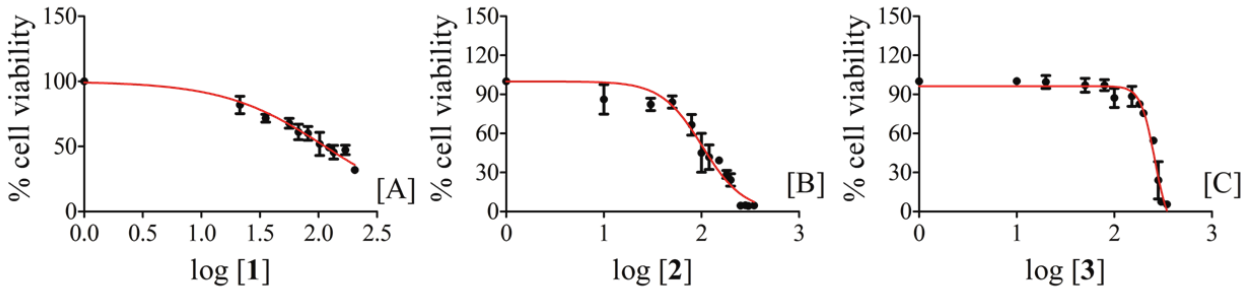

Fig. S1 Effects of treatment of the complexes **1-3** with MCF-7 tumor cell line for 48 h with rising concentrations: (A) **1**, (B) **2**, (C) **3**. The IC_{50} obtained from the curves are calculated using GraphPad Prism 5.0®. Data are mean ± SD of three independent experiments.

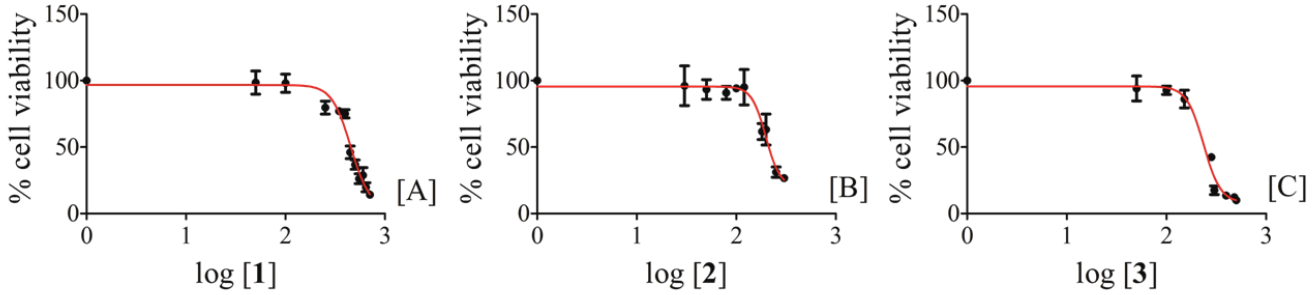

Fig. S2 Effects of treatment of the complexes **1-3** with A549 tumor cell line for 48 h with rising concentrations: (A) **1**, (B) **2**, (C) **3**. The IC_{50} obtained from the curves are calculated using GraphPad Prism 5.0®. Data are mean ± SD of three independent experiments.

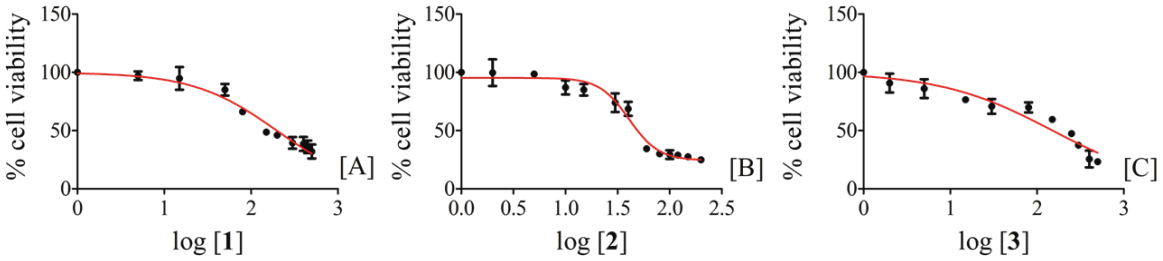

Fig. S3 Effects of treatment of the complexes **1-3** with NIH 3T3 tumor cell line for 48 h with rising concentrations: (A) **1**, (B) **2**, (C) **3**. The IC_{50} obtained from the curves are calculated using GraphPad Prism 5.0®. Data are mean ± SD of three independent experiments.

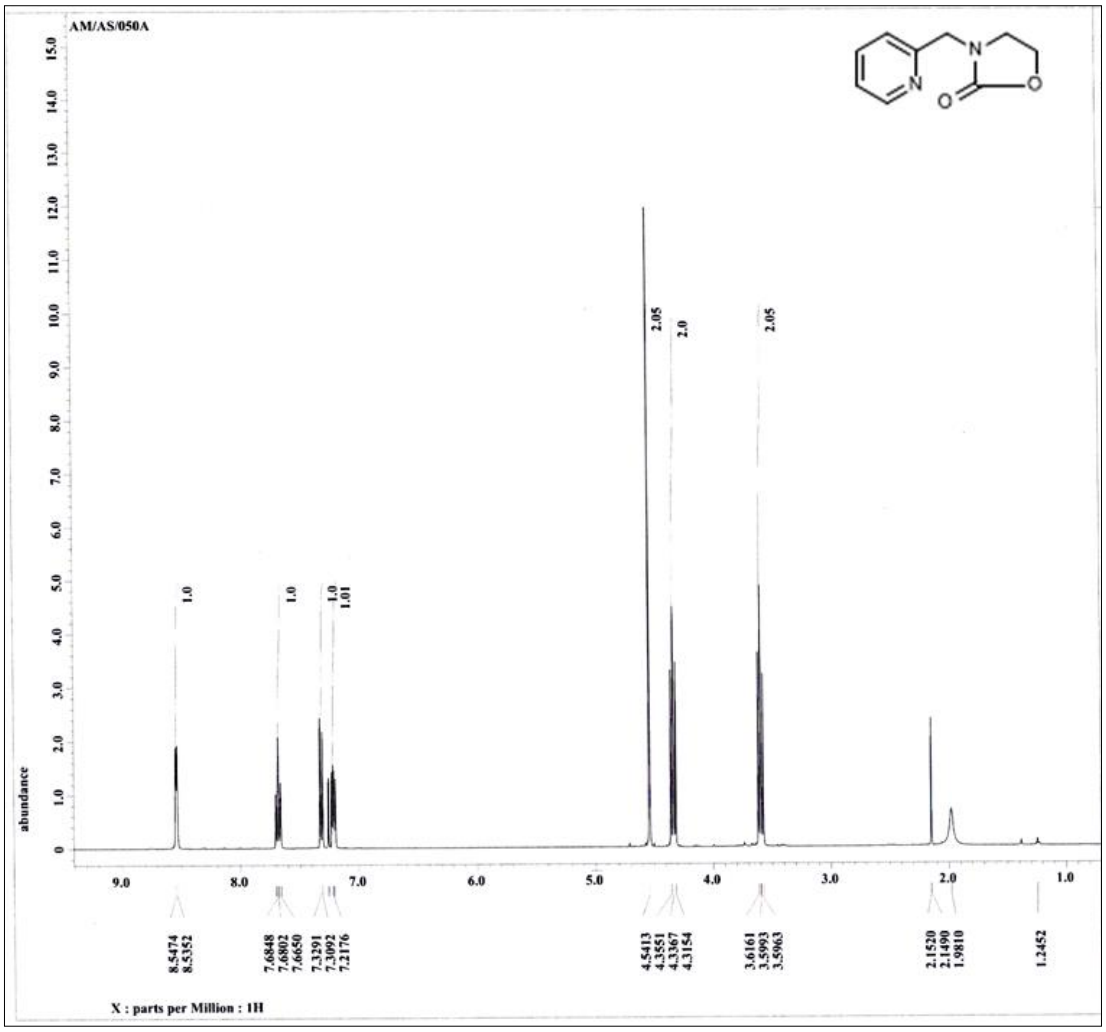

Fig. S4 ^{1}H-NMR of ligand L.

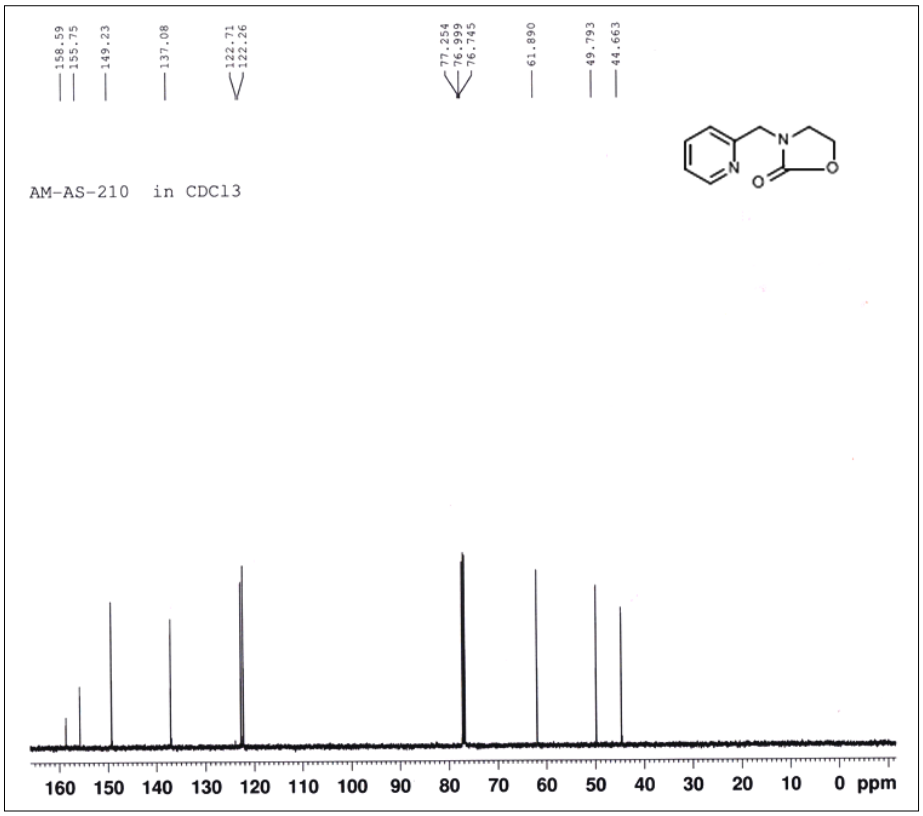

Fig. S5 ^{13}C-NMR of ligand L.

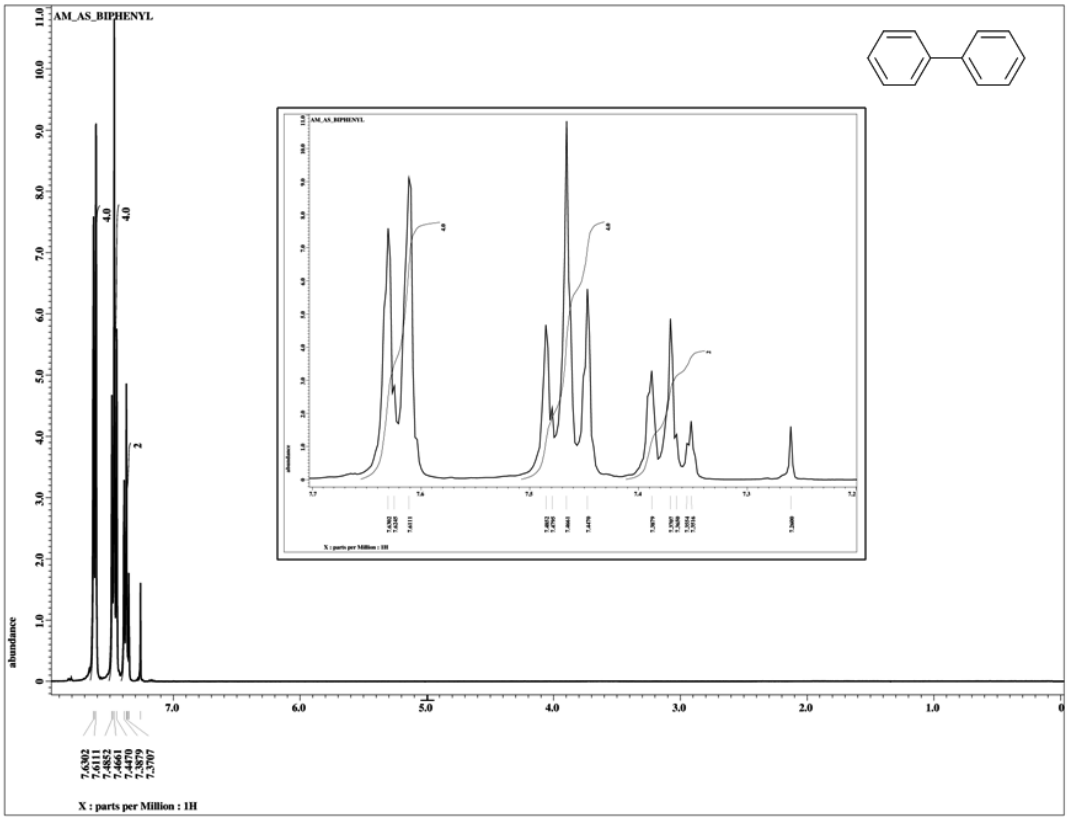

Fig. S6 ^{1}H-NMR of biphenyl in $CDCl_3$

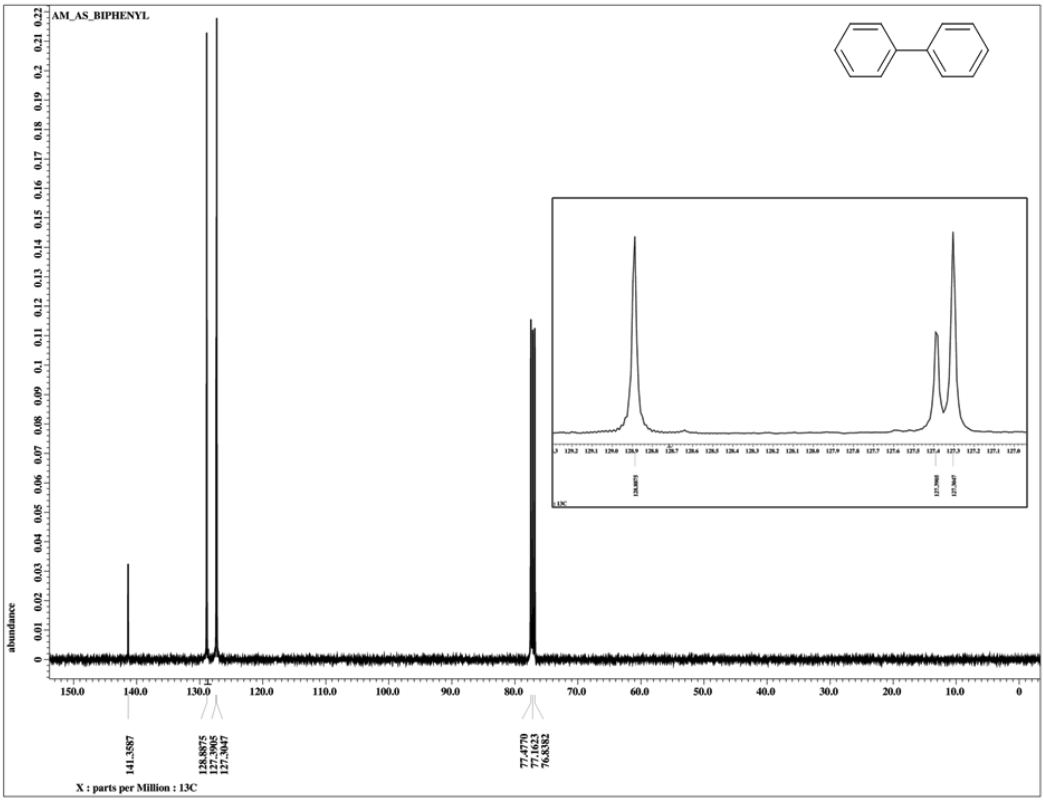

Fig. S7 ^{13}C-NMR of biphenyl in $CDCl_3$.

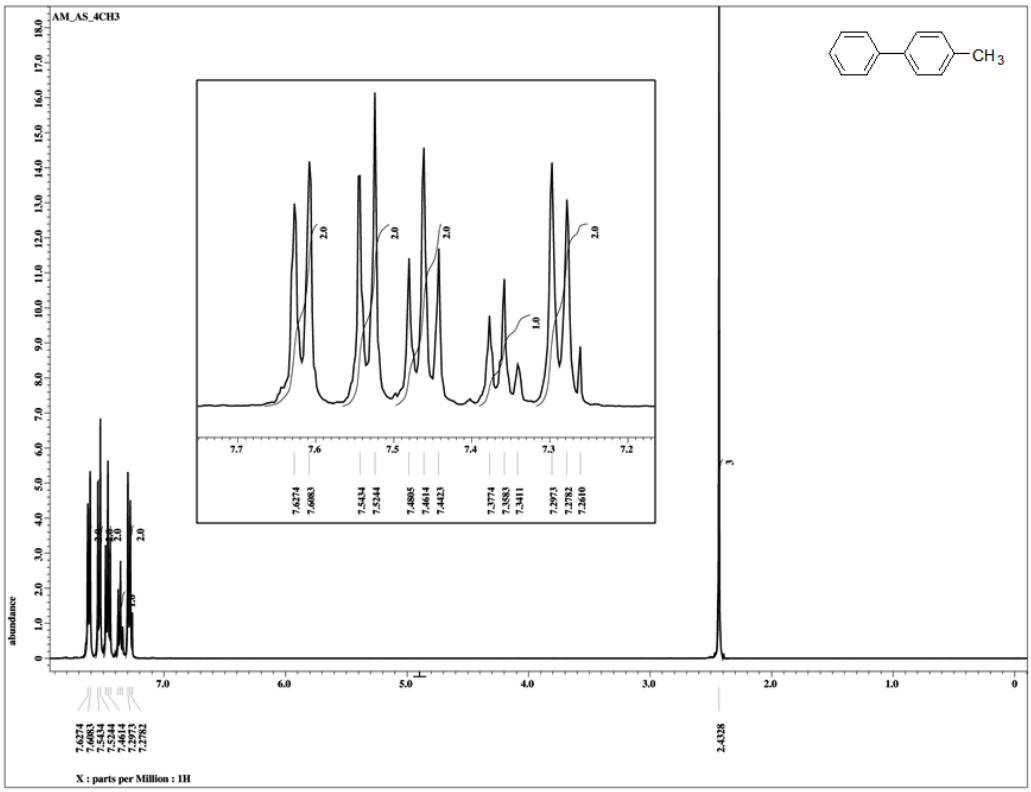

Fig. S8 ^{1}H-NMR of 4-methylbiphenyl in $CDCl_3$.

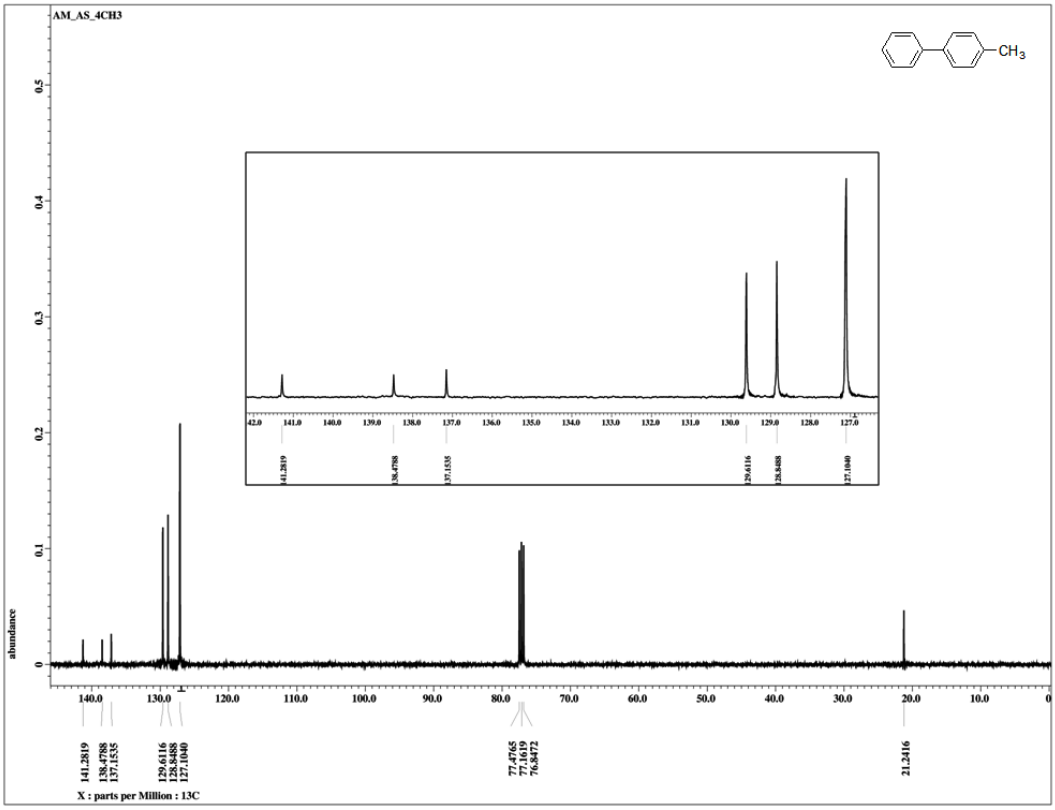

Fig. S9 ^{13}C-NMR of 4-methylbiphenyl in $CDCl_3$.

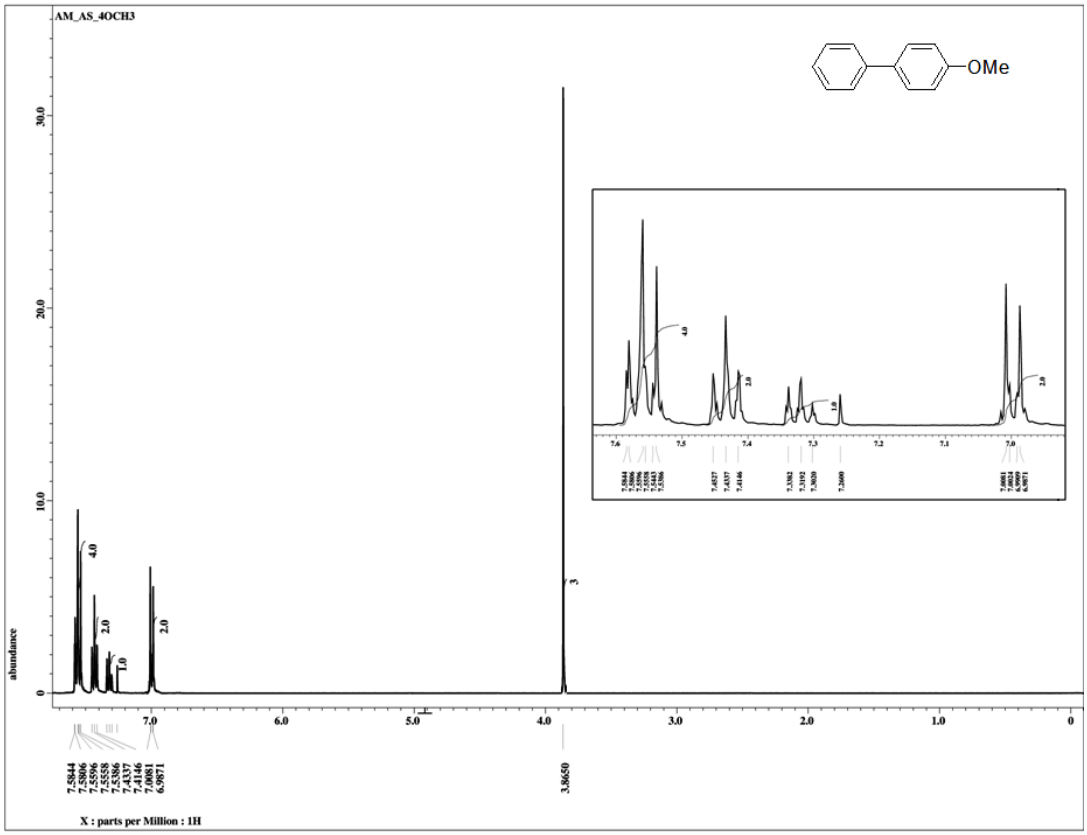

Fig. S10 ^{1}H-NMR of 4-methoxylbiphenyl in $CDCl_3$.

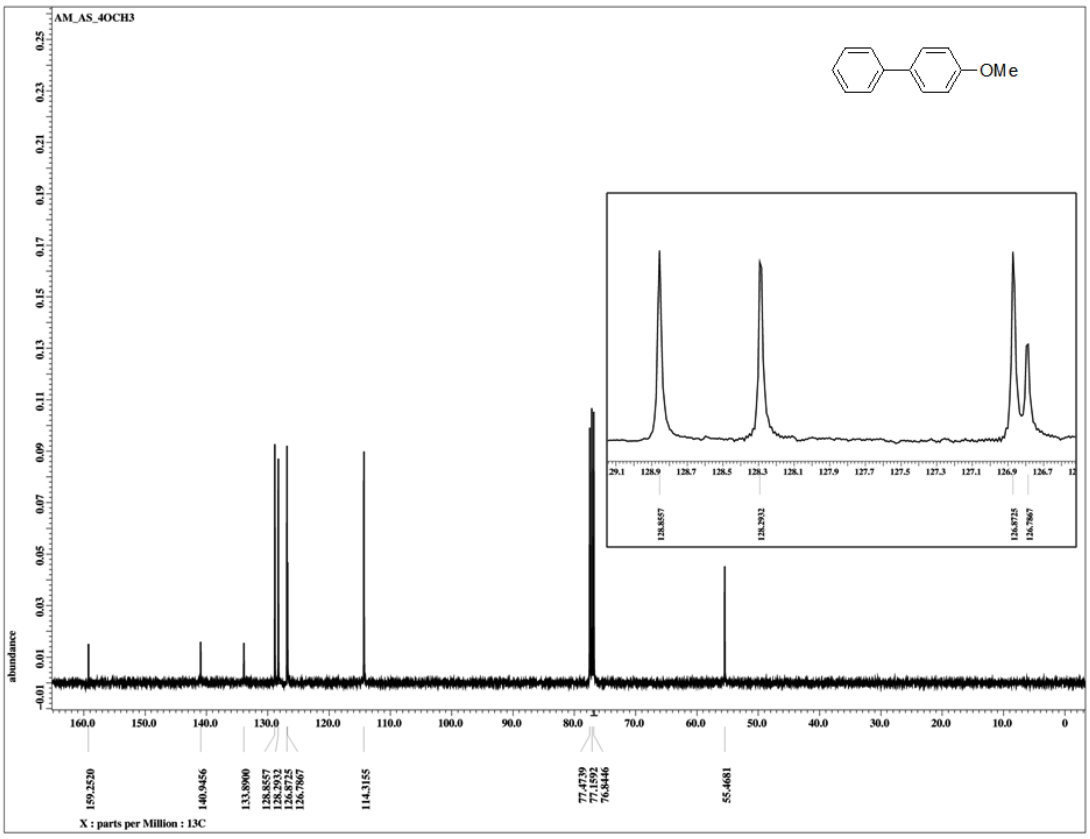

Fig. S11 ^{13}C-NMR of 4-methoxylbiphenyl in $CDCl_3$.

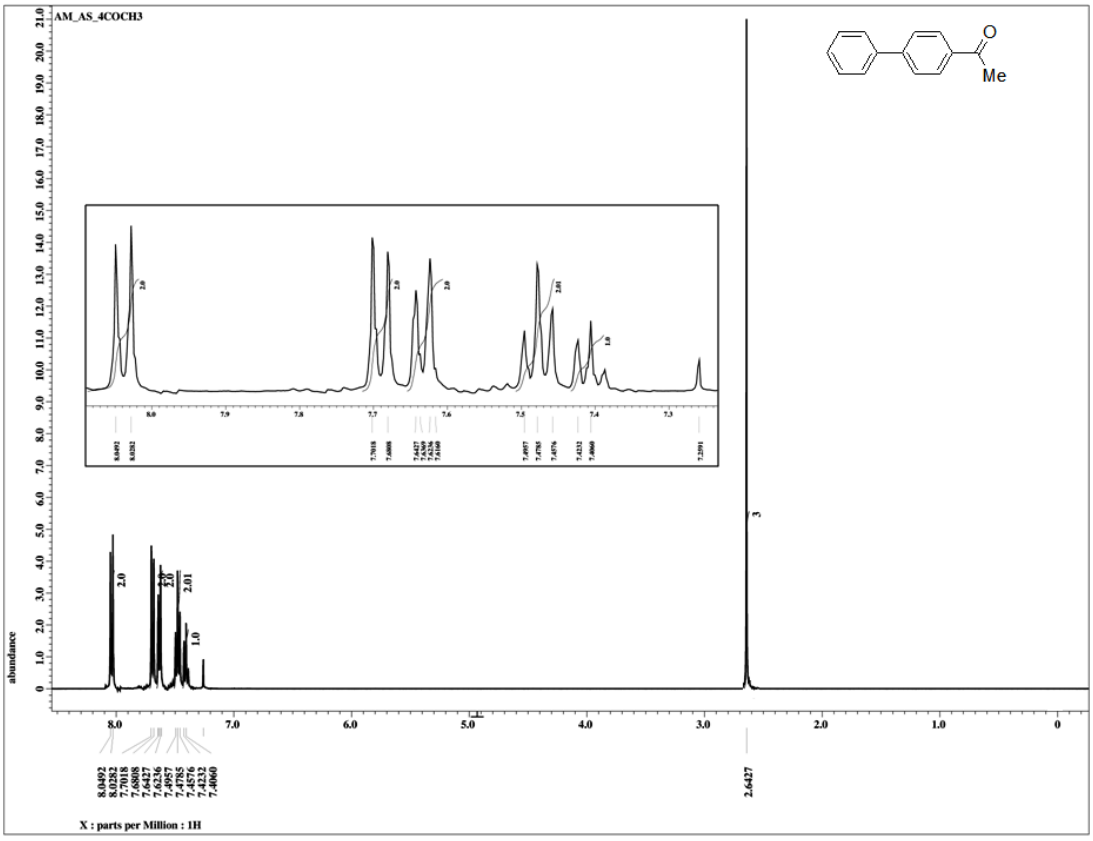

Fig. S12 ^{1}H-NMR of 4-acetylbiphenyl in $CDCl_3$.

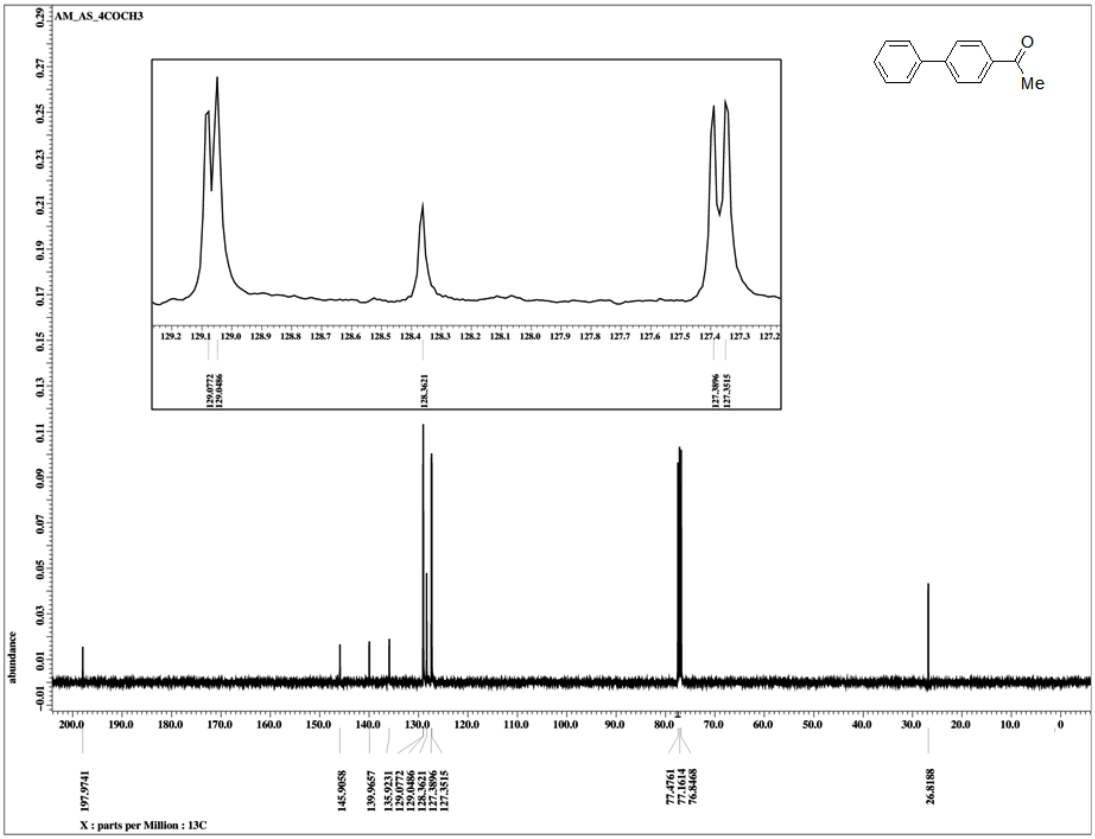

Fig. S13 ^{13}C-NMR of 4-acetylbiphenyl in $CDCl_3$.

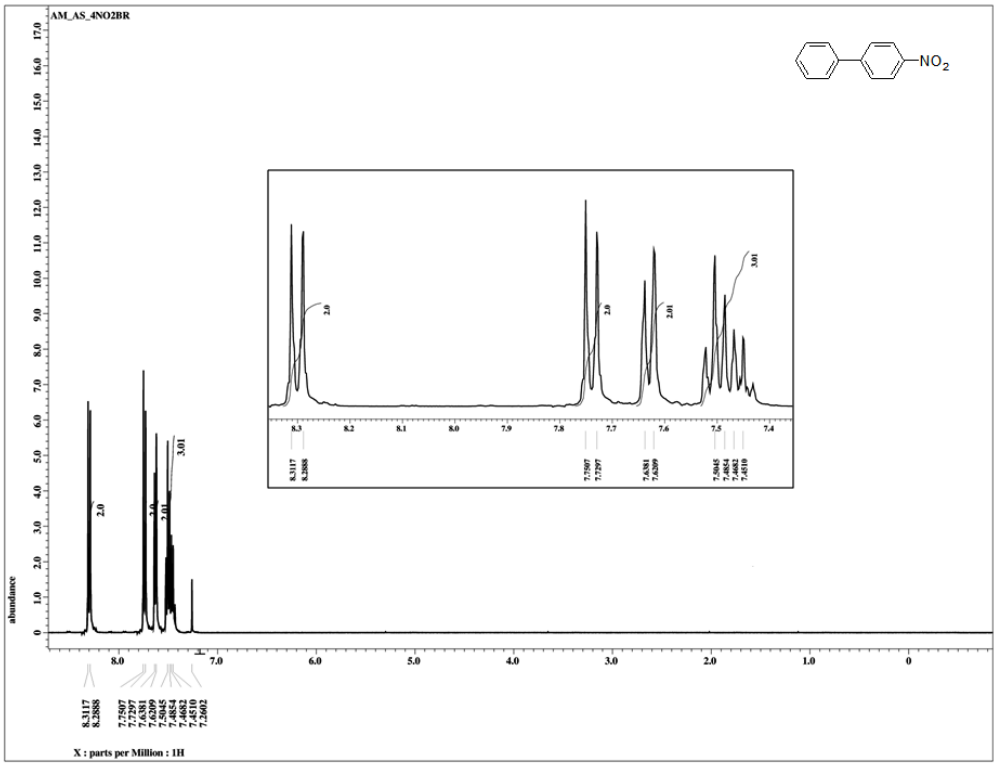

Fig. S14 ^{1}H-NMR of 4-nitrobiphenyl in $CDCl_3$.

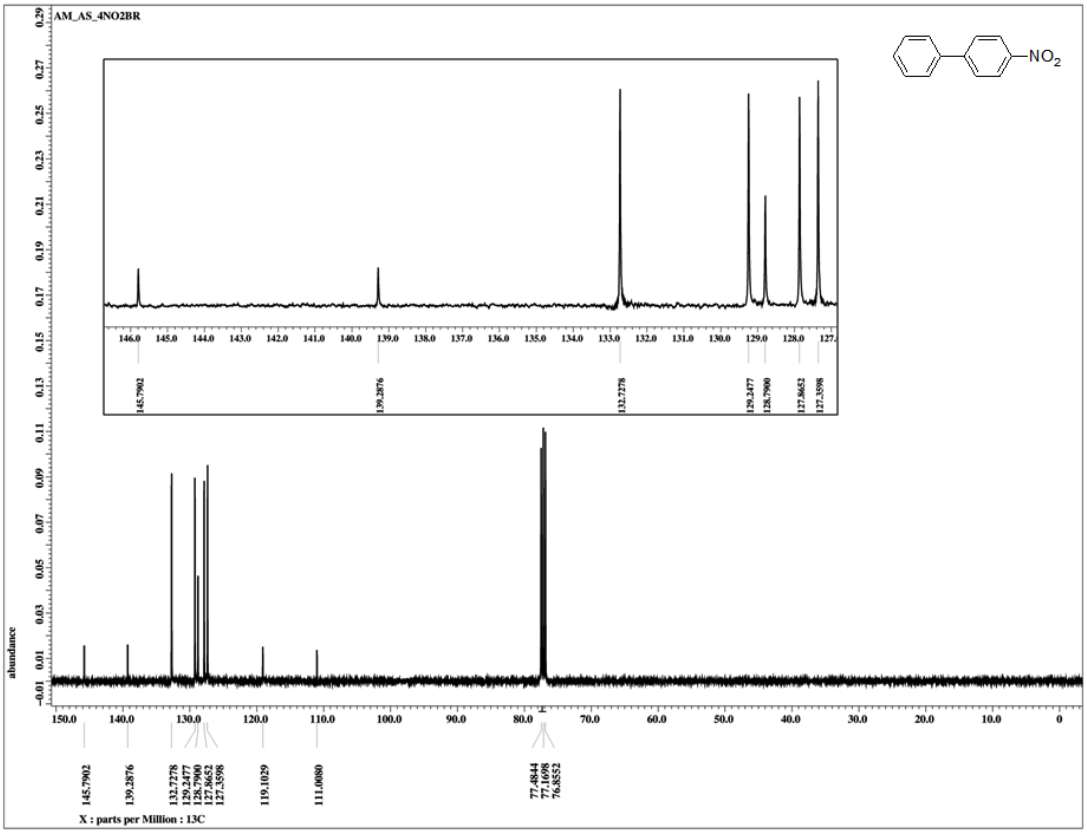

Fig. S15 ^{13}C-NMR of 4-nitrobiphenyl in $CDCl_3$.

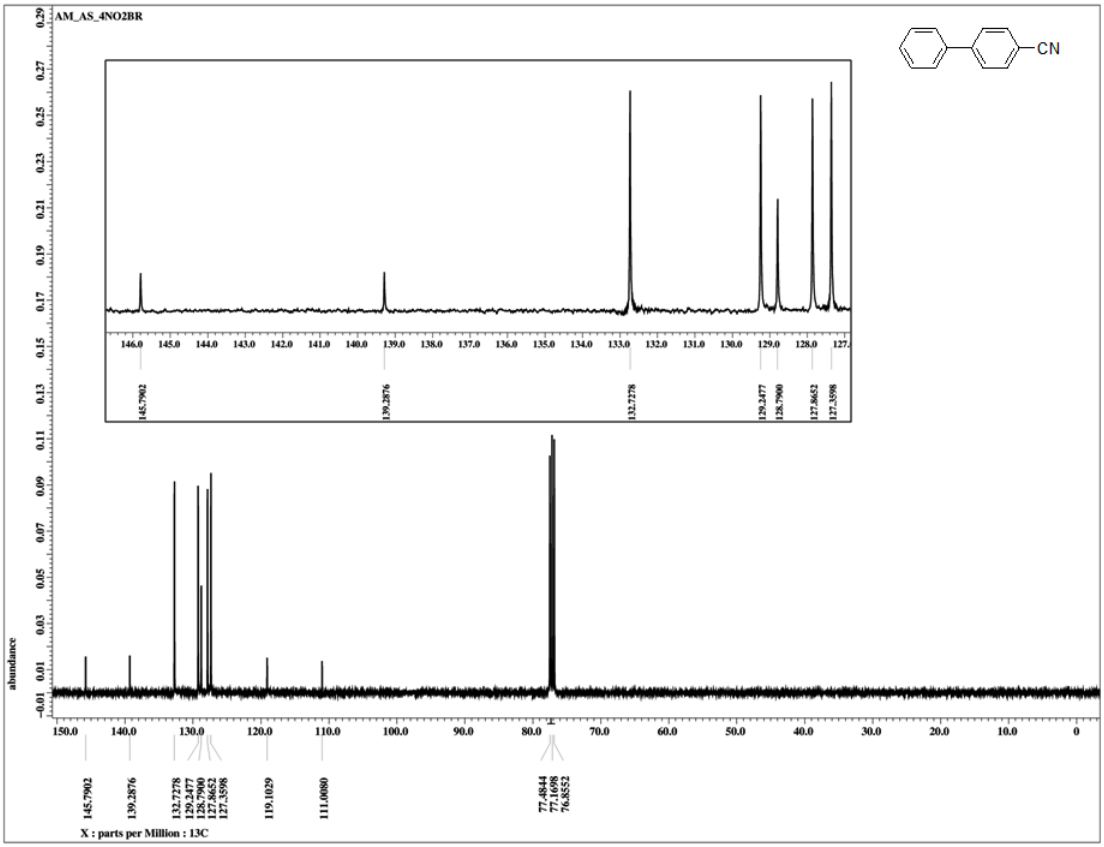

Fig. S16 ^{1}H-NMR of 4-cyanobiphenyl in $CDCl_3$.

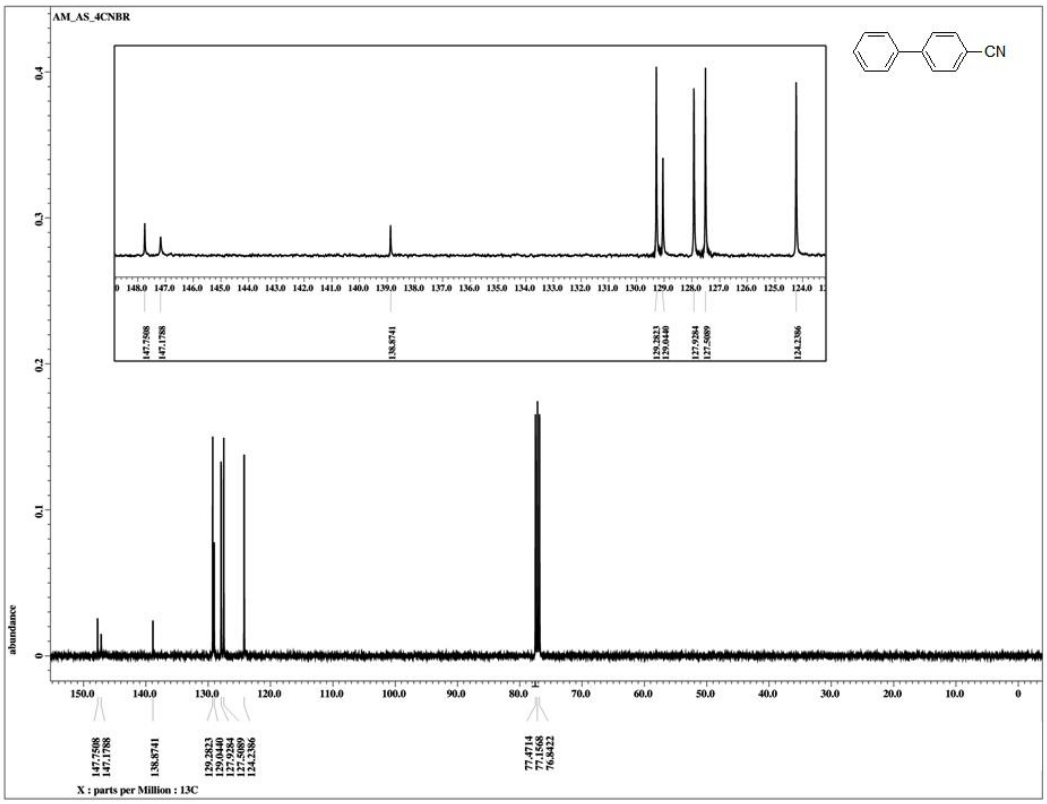

Fig. S17 ^{1}H-NMR of 4-cyanobiphenyl in $CDCl_3$.

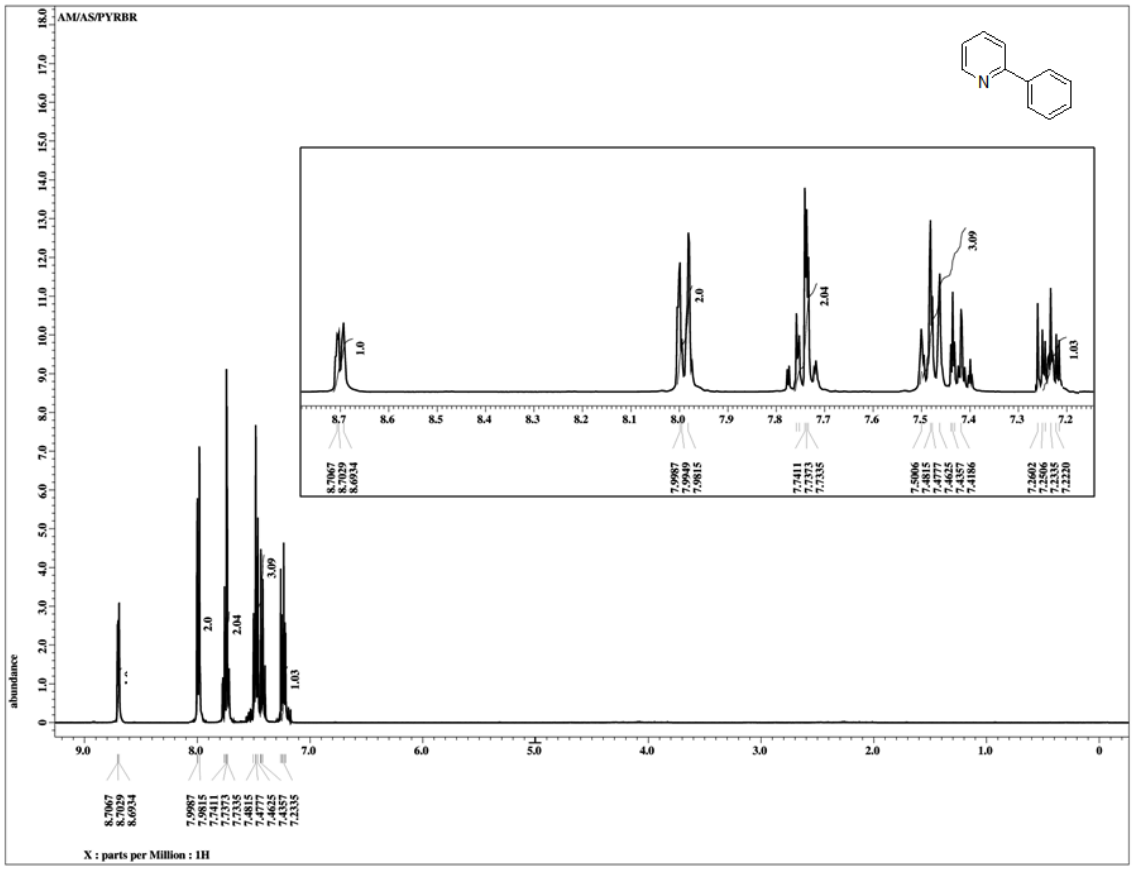

Fig. S18 ^{1}H-NMR of 2-phenylpyridine in $CDCl_3$.

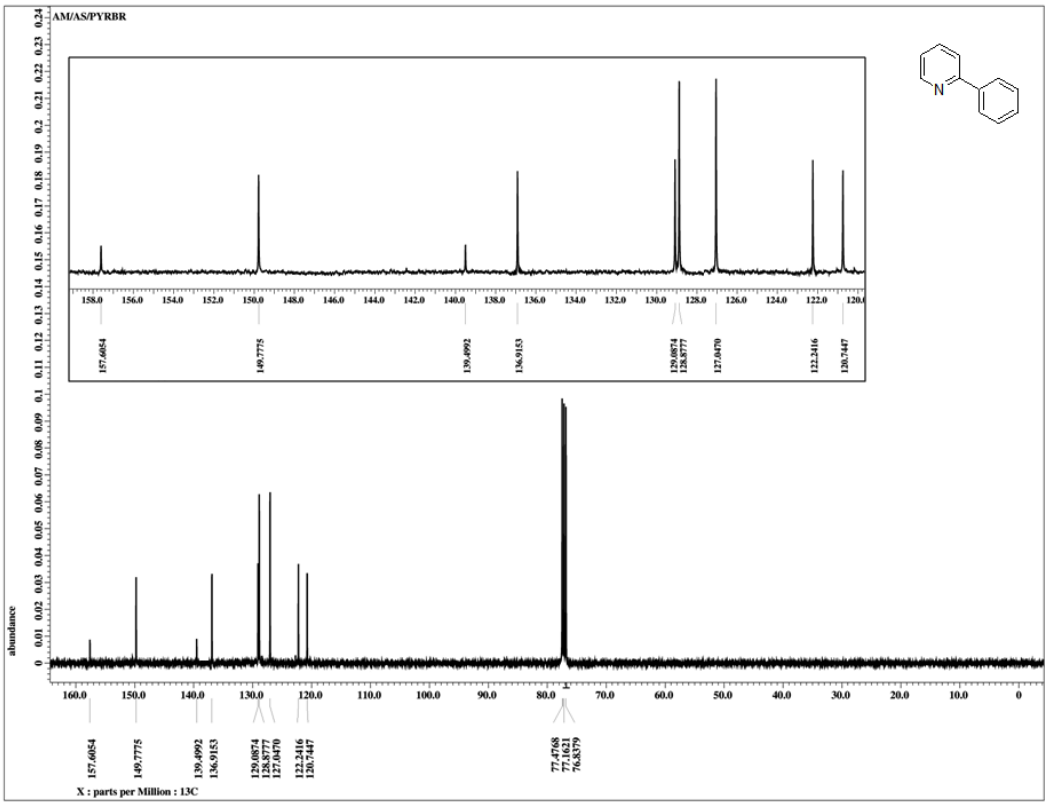

Fig. S19 ^{13}C-NMR of 2-phenylpyridine in $CDCl_3$.